

Differential Effects of Ontamalimab Versus Vedolizumab on Immune Cell Trafficking in Intestinal Inflammation and Inflammatory Bowel Disease

Lisa Lou Schulze^a, Emily Becker^a, Mark Dedden^a, Li-Juan Liu^a, Chiara van Passen^b,
Mariam Mohamed-Abdou^b, Tanja M. Müller^{a,c}, Maximilian Wiendl^a, Karen A.-M. Ullrich^a,
Imke Atreya^{a,c}, Moritz Leppkes^{a,c}, Arif B. Ekici^d, Philipp Kirchner^d, Michael Stürzl^b,
Dan Sexton^e, Deborah Palliser^e, Raja Atreya^{a,c}, Britta Siegmund^{f, },
TRR241 IBDome consortium^g, Markus F. Neurath^{a,c}, Sebastian Zundler^{a,c, }

^aDepartment of Medicine 1, University Hospital Erlangen and Friedrich-Alexander-Universität Erlangen-Nürnberg, Germany

^bDepartment of Surgery, Division of Molecular and Experimental Surgery, University Hospital Erlangen and Friedrich-Alexander Universität Erlangen-Nürnberg, Germany

^cDeutsches Zentrum Immuntherapie (DZI), University Hospital Erlangen, Germany

^dInstitute of Human Genetics, University Hospital Erlangen and Friedrich-Alexander-Universität Erlangen-Nürnberg, Germany

^eShire HGT, a Takeda company, Cambridge, MA, USA

^fDivision of Gastroenterology, Infectiology and Rheumatology, Charité – Universitätsmedizin Berlin, corporate member of Freie Universität Berlin and Humboldt-Universität zu Berlin, Berlin, Germany

^gTRR241 research initiative, Charité Universitätsmedizin Berlin and University Hospital Erlangen, Germany

Corresponding author: Sebastian Zundler, MD, PhD, Department of Medicine 1, Friedrich-Alexander Universität Erlangen-Nürnberg, Ulmenweg 18, D-91054 Erlangen, Germany. Tel: 49-9131-85-35000; Fax: 49-9131-85-35209; Email: sebastian.zundler@uk-erlangen.de

Abstract

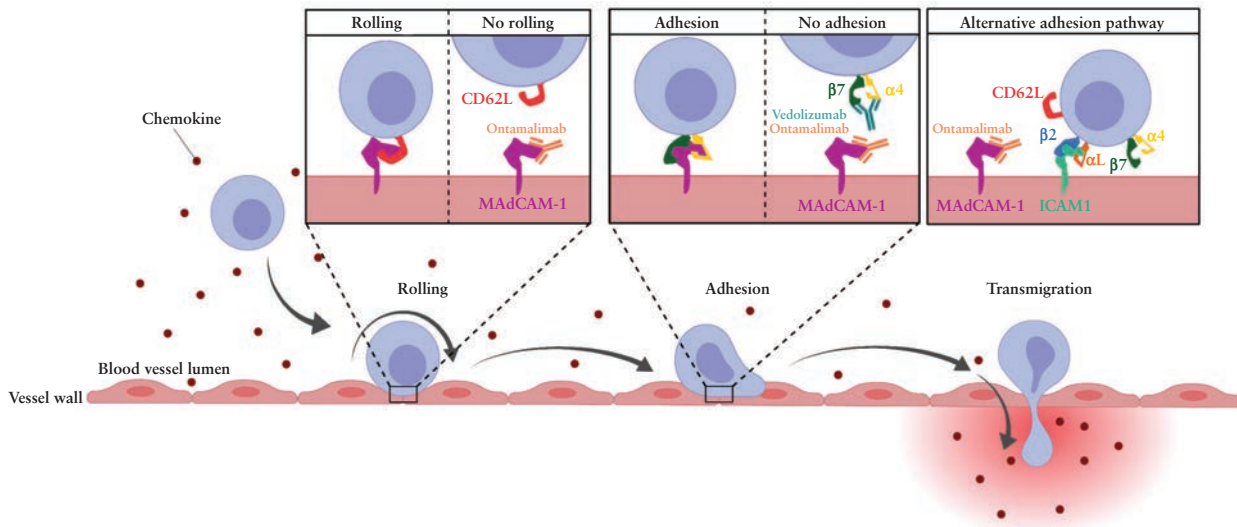
Background and Aims: The anti-MAdCAM-1 antibody ontamalimab demonstrated efficacy in a phase II trial in ulcerative colitis and results of early terminated phase III trials are pending, but its precise mechanisms of action are still unclear. Thus, we explored the mechanisms of action of ontamalimab and compared it to the anti- $\alpha 4\beta 7$ antibody vedolizumab.

Methods: We studied MAdCAM-1 expression with RNA sequencing and immunohistochemistry. The mechanisms of action of ontamalimab were assessed with fluorescence microscopy, dynamic adhesion and rolling assays. We performed *in vivo* cell trafficking studies in mice and compared ontamalimab and vedolizumab surrogate [-s] antibodies in experimental models of colitis and wound healing. We analysed immune cell infiltration under anti-MAdCAM-1 and anti- $\alpha 4\beta 7$ treatment by single-cell transcriptomics and studied compensatory trafficking pathways.

Results: MAdCAM-1 expression was increased in active inflammatory bowel disease. Binding of ontamalimab to MAdCAM-1 induced the internalization of the complex. Functionally, ontamalimab blocked T cell adhesion similar to vedolizumab, but also inhibited L-selectin-dependent rolling of innate and adaptive immune cells. Despite conserved mechanisms in mice, the impact of ontamalimab-s and vedolizumab-s on experimental colitis and wound healing was similar. Single-cell RNA sequencing demonstrated enrichment of ontamalimab-s-treated lamina propria cells in specific clusters, and *in vitro* experiments indicated that redundant adhesion pathways are active in these cells.

Conclusions: Ontamalimab has unique and broader mechanisms of action compared to vedolizumab. However, this seems to be compensated for by redundant cell trafficking circuits and leads to similar preclinical efficacy of anti- $\alpha 4\beta 7$ and anti-MAdCAM-1 treatment. These results will be important for the interpretation of pending phase III data.

Graphical Abstract



1. Introduction

Immune cell homing to the gut is considered as an important aspect of the pathogenesis of the inflammatory bowel diseases [IBD] Crohn's disease [CD] and ulcerative colitis [UC].^{1,2} Consistently, therapies interfering with immune cell trafficking pathways such as the anti- $\alpha 4\beta 7$ integrin antibody vedolizumab or the sphingosine-1 phosphate receptor [S1PR] agonist ozanimod have been developed and approved for therapy of patients with IBD after demonstration of efficacy and safety in phase III trial programmes.^{3–5}

In addition, several other anti-trafficking agents have been designed and tested in preclinical animal models as well as in clinical trials in patients with IBD.⁶ One of them is the antimucosal addressin cell adhesion molecule [MAdCAM]-1 antibody ontamalimab [formerly also known as PF-00547659 and SHP647].⁷ Ontamalimab is a fully human monoclonal antibody selectively binding to the N-terminal tip of the D1 domain of MAdCAM-1, and thus blocking the binding of $\alpha 4\beta 7$ integrin to this site.⁸

MAdCAM-1 is almost exclusively expressed on high endothelial venules of the gut and the gut-associated lymphoid system.⁹ It has important functions in the multistep cascade of gut homing. Specifically, gut-homing immune cells expressing L-selectin [CD62L] or an inactive conformation of $\alpha 4\beta 7$ integrin loosely interact with MAdCAM-1 resulting in a rolling behaviour that slows down the cells along the vessel wall.¹⁰ On exposure to tissue-derived chemokines activating intracellular signalling pathways via G protein-coupled receptors, $\alpha 4\beta 7$ integrin undergoes conformational changes resulting in an open, active configuration mediating firm binding to MAdCAM-1 and facilitating subsequent transendothelial migration.^{11,12} While the interaction of $\alpha 4\beta 7$ with MAdCAM-1 is considered quite specific for the gut, similar interactions such as $\alpha 4\beta 1$ integrin with vascular cell adhesion molecule [VCAM]-1 or $\alpha L\beta 2$ integrin with intercellular adhesion molecule [ICAM]-1 can also mediate homing to the intestine.¹³

Ontamalimab has previously been investigated in phase II clinical trials for UC and CD. While the TURANDOT trial in UC demonstrated higher remission rates at week 12 with ontamalimab compared with placebo,¹⁴ outcomes in the OPERA trial in CD did not differ between ontamalimab and

placebo.¹⁵ The reasons for these discrepant results are unclear so far.

Moreover, since both vedolizumab and ontamalimab block the interaction of $\alpha 4\beta 7$ integrin with MAdCAM-1, it has been under debate, whether—despite different molecular targets—the actual mechanism of the two antibodies might really differ.^{16–18} However, in practice, the mechanism of action of ontamalimab has previously not been investigated in detail and has not been compared to vedolizumab.

Thus, the aim of this study was to explore the precise mechanism of ontamalimab and to compare it with vedolizumab. We show that, in contrast to vedolizumab, ontamalimab blocks interactions of MAdCAM-1 with L-selectin in addition to MAdCAM-1- $\alpha 4\beta 7$ ligation and therefore interferes with cell trafficking pathways of several innate immune cells. However, this did not result in differential outcomes across several experimental models of colitis and wound healing, probably due to evasion of ontamalimab-specific mechanisms via redundant pathways. Thus, ontamalimab has a distinct mechanism of action that is different from and broader than that of vedolizumab, but might not lead to improved inhibition of cell trafficking.

2. Materials and Methods

Key methods are described in the following paragraphs. Additional methods are available in the [Supplementary File](#).

2.1. Patients and samples

Peripheral blood samples and gut tissue were obtained from patients with CD or UC as well as from healthy controls at the Department of Medicine 1 of the University Hospital Erlangen after written informed consent. Patients who had previously received vedolizumab were not included. Moreover, *MADCAM1* mRNA expression and correlation analyses were performed within the IBDome RNA sequencing [RNA-seq] database of the Transregio Collaborative Research Unit 241.

The procedures were approved by the Ethics Committee of the Friedrich-Alexander-Universität Erlangen-Nürnberg. Patients' characteristics are summarized in [Table 1](#).

Table 1. Patient characteristics

	Non-IBD	CD	UC
Number	50	38	42
Age, years [mean, range]	30.7 [20–79]	38.9 [20–85]	42.6 [20–77]
Female [%]	82	42.1	45.2
HBI [mean, range]		3.29 [1–10]	
Mayo Score [mean, range]			2.04 [0–10]
Therapy [%]	Aminosalicylates	13.2	34.2
	Steroids	5.3	18.4
	Immunosuppressants	7.9	13.2
	Anti-TNF antibodies	68.4	57.9
	Vedolizumab	2.6	21.1
	Ustekinumab	13.2	5.3
Disease localization [%]		L1: 21.1	E1: 20
		L2: 18.4	E2: 17.5
		L3: 60.5	E3: 62.5
		L4: 0	
		L4+: 31.6	

IBD, inflammatory bowel disease; CD, Crohn's disease; UC, ulcerative colitis; HBI, Harvey–Bradshaw Index; TNF, tumour necrosis factor.

2.2. Dynamic *in vitro* adhesion assays

Fc chimera of either recombinant human [rh] MAdCAM-1, rh ICAM-1 or recombinant mouse [rm] MAdCAM-1 [R&D Systems] were used to coat the inside of miniature borosilicate capillaries [Vitrocom] at a concentration of 5 µg/mL in 150 mM NaCl with 10 mM HEPES [VWR] for 1 h at 37°C. Unspecific binding sites were blocked with 10% fetal calf serum [FCS] in phosphate buffered saline [PBS] for 1 h at 37°C. Capillaries were connected to plastic tubing that was inserted into a peristaltic pump [Baoding Shenchen] with adjustable flow rate. Cells were fluorescently stained with carboxyfluorescein succinimidyl ester [CFSE; Life Technologies] and resuspended in adhesion buffer [pH 7.4; 150 mM NaCl, 10 mM HEPES, 1 mM CaCl₂, 1 mM MgCl₂, 1 mM MnCl₂] at a concentration of 1.5 × 10⁶ cells/mL. The antibodies vedolizumab [anti-α4β7; Takeda] or ontamalimab [anti-MAdCAM-1; Shire] were added to human cells, whereas the surrogate antibodies DATK32 [anti-α4β7¹⁹] or MECA367 [anti-MAdCAM-1; both Bio X Cell] were added to mouse cells at a concentration of 10 µg/mL directly prior to perfusion. Labelled and treated cells were perfused through the capillaries at a flow rate of 10 µL/min for 3 min. Afterwards, the capillaries were rinsed with adhesion buffer at a flow rate of 50 µL/min for 5 min. Adherent cells were quantified using an inverted microscope [DMI8; Leica].

2.3. *In vitro* rolling assays

Fc chimera of either rh MAdCAM-1 [R&D Systems], rh VCAM-1 [BioLegend] or rm MAdCAM-1 [R&D Systems] were coated into flow chambers [µ-Slide I Luer; ibidi] at a concentration of 5 µg/mL in 150 mM NaCl with 10 mM HEPES. Coating solution was replaced by 10% FCS in PBS to block unspecific binding sites. Cells were fluorescently stained with CFSE and resuspended in adhesion buffer without MnCl₂ at a concentration of 0.5 × 10⁶ cells/mL. Flow chambers were connected to plastic tubing inserted into a peristaltic pump and placed on a confocal microscope [SP8; Leica]. Vedolizumab, ontamalimab or anti-CD62L antibodies [absolute antibody]

were added to human cells, whereas DATK32 or MECA367 were added to mouse cells at a concentration of 10 µg/mL directly prior to perfusion. During perfusion, time-lapse confocal videos of 2 min in length were recorded for each flow chamber. ImageJ [NIH] TrackMate software was used to determine mean velocities of 30 cells per video.

2.4. *In vivo* gut homing experiments

Rag1^{-/-} mice were given 1.5% dextran sodium sulphate [DSS; MP Biomedicals] in their drinking water for 7 days to induce mild colitis. CD4⁺ T cells from the spleens of C57BL/6J, B6;129S2-Sell<tm2Hyn>/J [*Sell*^{-/-}], C57BL/6-Itgb7<tm1Cgn>/J [*Itgb7*^{-/-}] and *Sell*^{-/-}*Itgb7*^{-/-} donor mice were isolated and fluorescently labelled with CellTrace™ Far Red [Invitrogen]. Up to 4 × 10⁶ cells were intravenously [i.v.] injected into the tail vein of the *Rag1*^{-/-} mice. C57BL/6J cells were injected together with either rat IgG isotype control antibody, DATK32 or MECA367. The mice were killed 24 h later and lamina propria mononuclear cells [LPMCs] were isolated for flow cytometry.

2.5. Acute DSS colitis

C57BL/6J mice were treated with 1.5% DSS in their drinking water for 7 days, followed by 3 days of normal drinking water. Mice were treated with 250 µg of MECA-367, DATK32 or rat IgG isotype control antibody intraperitoneally [i.p.] three times a week. Mini-endoscopy and LPMC isolation were performed as described above.

2.6. Single cell sequencing

LPMCs from C57BL/6J mice with acute DSS-colitis treated with DATK32, MECA367 or rat IgG were stained for viability [Fixable Viability Dye eFluor™ 780; Invitrogen] and CD45 [clone 30-F11; Biolegend]. FcR Blocking Reagent [murine; Miltenyi] was used to inhibit unspecific antibody binding. Using fluorescence activated cell sorting [FACS] on a MoFlo Astrios EQ [Beckman Coulter], viable CD45⁺ LPMCs were separated. Cells were further prepared for single cell sequencing

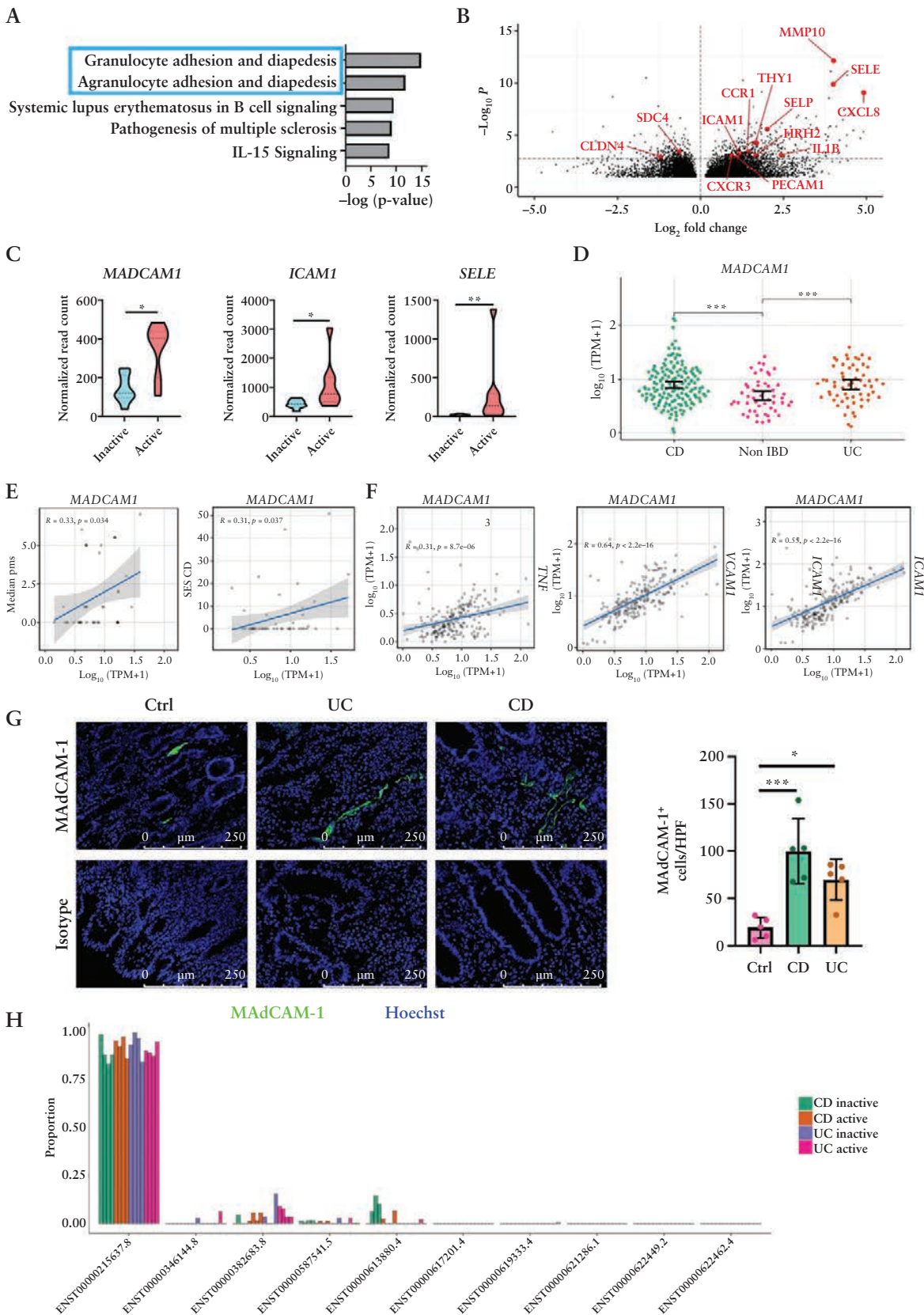


Figure 1. Increased expression of MAdCAM-1 in active IBD. [A–C] Bulk RNA-sequencing of colon tissue from eight patients with UC [four inactive, four active] and eight patients with CD [four inactive, four active]. [A] Top five differentially regulated pathways between patients with active and inactive disease as identified by Ingenuity Pathway Analysis. [B] Volcano plot highlighting selected genes from the adhesion and diapedesis pathways identified in A differentially expressed between patients with inactive vs active disease. [C] Normalized read count of selected adhesion-associated genes in patients with inactive and active disease. [D–F] Analyses based on transcriptomic profiling of biopsies from patients with IBD and controls within the TRR241 IBDome consortium. [D] Expression of *MADCAM1* in patients with CD ($n = 150$), UC ($n = 60$) or without IBD ($n = 51$). [E] Correlation

according to the instructions for the Chromium Next GEM Single Cell 3' Reagent Kit v.3.1 from 10x Genomics. The libraries were shipped to GeneWiz for sequencing. All samples were sequenced together in one Illumina® NovaSeq™ 6000 lane, reaching an average of 85 million reads per sample and raw data were delivered in FASTQ format. Subsequently, Cell Ranger v.6.0.2 was invoked to align the reads against the mouse reference genome mm10 and to output a single cell gene expression matrix. Downstream analysis of the gene expression matrix was performed with Scanpy v.1.7.2, using Python v.3.6 in a Jupyter Notebook environment v.6.3.0.

All cells with a mitochondrial content higher than 20% were filtered out, as well as cells with fewer than 500 unique molecular identifiers (UMIs), fewer than 250 genes or more than 30 000 UMIs. Normalization of the UMI counts was achieved through size factor correction using DeSeq2 v.1.24.0 in R v.3.6.1. For the purpose of clustering, dimension reduction was performed by Uniform Manifold Approximation and Projection [UMAP] and the Leiden algorithm was applied to detect communities.

At a resolution of 0.5 Leiden, the clusters enriched for CD45 expression were selected and the remaining cells were normalized and another UMAP dimension reduction and Leiden community detection was performed.

2.7. Animals

C57BL/6J [WT], B6.129S7-Rag1<tm1Mom>/J [*Rag1*^{-/-}], B6;129S2-Sell<tm2Hyn>/J [*Sell*^{-/-}], C57BL/6-Itgb7<tm1Cgn>/J [*Itgb7*^{-/-}] and *Sell*^{-/-}*Itgb7*^{-/-} double knockout mice were housed in individually ventilated cages

with a regular day–night cycle and used for experiments according to approval of the Government of Lower Franconia in compliance with all relevant ethical regulations.

2.8. Statistics

All statistical analysis was performed using the GraphPad Prism software v.9.0.2. In order to choose the appropriate statistical [parametric or non-parametric] tests, the Shapiro–Wilk test was used to test all data for normal distribution. If the data were normally distributed, a paired or unpaired *t*-test was used to analyse two groups as appropriate. If more than two groups were analysed, a one-way ANOVA was performed with a Tukey or Dunnett's post-hoc test, if not otherwise indicated. In case of not normally distributed data, the Mann–Whitney test was used to analyse two groups. For the analysis of more than two groups the Kruskal–Wallis test with Dunn's post-hoc test was chosen. For the analysis of more than two groups, which are dependent on an additional variable, a two-way ANOVA was calculated with Tukey's multiple comparison post-hoc test. Outliers were identified using Grubb's test, where indicated. Error bars in all graphs display standard deviation. Probability values are indicated as follows: **p* < 0.05, ***p* < 0.01, ****p* < 0.001, *****p* < 0.0001.

3. Results

3.1. Cell trafficking pathways and MAdCAM-1 are upregulated in severe IBD

To interrogate the mechanisms driving inflammation in IBD, we performed paired-end bulk RNA-seq from colon

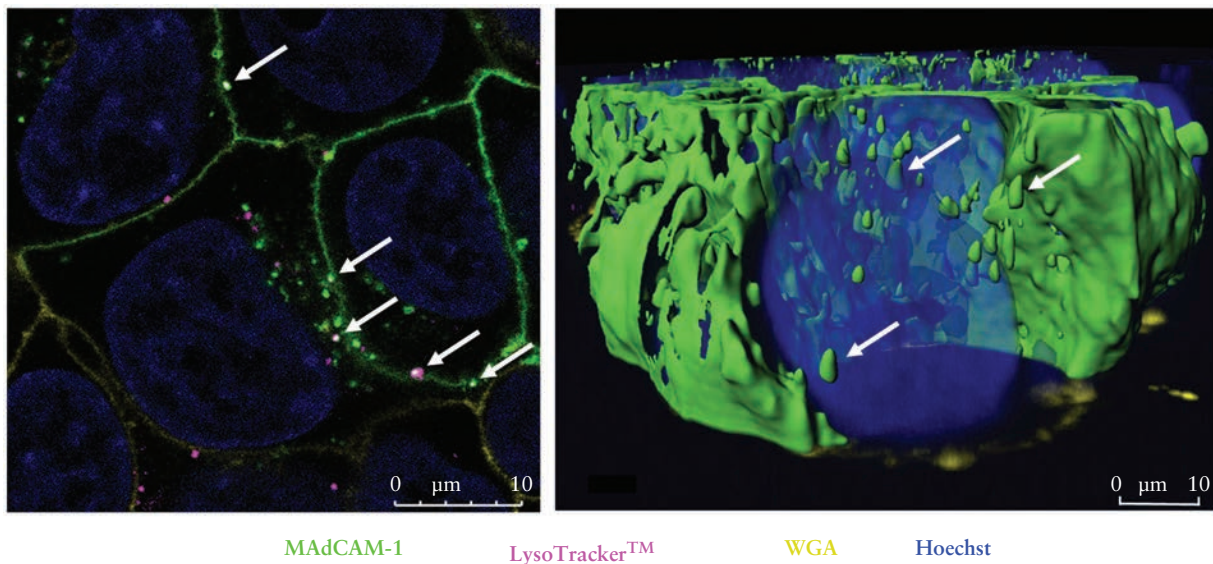


Figure 2. Ontamalimab binding leads to internalization of MAdCAM-1. Confocal microscopy demonstrating MAdCAM-1 internalization upon ontamalimab binding. MAdCAM-1-overexpressing HEK293T cells were incubated with fluorescently labelled ontamalimab [AF488, green]. Cell membranes [WGA-AF555, yellow], lysosomes [Lyso-Tracker 647, pink] and nuclei [Hoechst, blue] were additionally stained. Images are representative of five independent experiments.

of *MADCAM1* expression with the partial Mayo Score [pms] and the SES-CD in patients with UC and CD, respectively. [F] Correlation of *MADCAM1* expression with *TNF*, *VCAM1* and *ICAM1* expression. [G] Immunofluorescence staining of MAdCAM-1 on cryopreserved sections of human colon from patients with CD [*n* = 5], UC [*n* = 5] and healthy controls [*n* = 5]. Outliers were identified using Grubb's test. [H] Proportions of *MADCAM1* transcripts in the RNA sequencing data presented in A–C. CD, Crohn's disease; HBI, Harvey–Bradshaw Index; PMS, partial Mayo score; TPM, transcripts per million; UC, ulcerative colitis. **p* < 0.05, ***p* < 0.01, ****p* < 0.001.

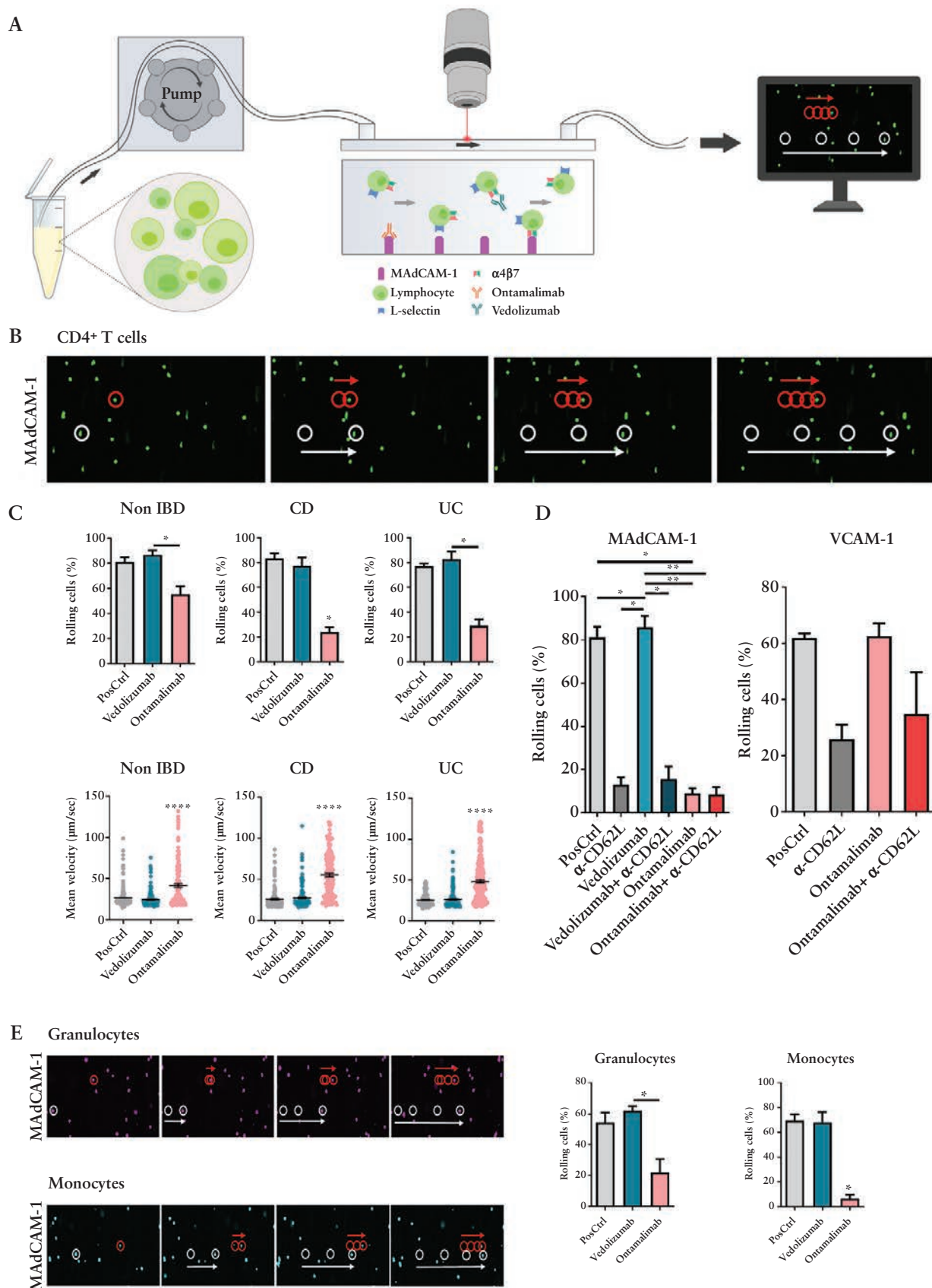


Figure 3. Ontamalimab blocks rolling of adaptive and innate immune cells on MAdCAM-1. [A] Schematic depiction of experimental setup. Cells of interest were perfused through MAdCAM-1-coated flow chambers and treated with different antibodies. Rolling was analysed by time-lapse confocal microscopy. [B] Representative time-lapse microscopy of CD4⁺ T cells perfused through the flow chamber highlighting a rolling [red] and a non-rolling cell [white]. [C] Fraction of rolling CD4⁺ T cells [upper panels] and mean velocity of CD4⁺ T cells [lower panels] from healthy donors and patients with CD

biopsies of eight patients with UC and eight patients with CD. We compared the transcriptome of patients who had active compared with inactive disease and performed Ingenuity Pathway Analysis [IPA] with differentially expressed genes. We found that ‘Granulocyte Adhesion and Diapedesis’ and ‘Agranulocyte Adhesion and Diapedesis’ were the two top regulated canonical pathways [Figure 1A]. Consistently, numerous genes known to be involved in cell trafficking pathways were differentially expressed in active compared with inactive IBD [Figure 1B], such as *MADCAM1*, *ICAM1* or *SELE* [Figure 1C].

We further investigated the expression of *MADCAM1* in the multi-centric IBDome database pooling transcriptomic data from the gut tissue of patients with IBD. In agreement with previous literature,^{20,21} the expression of *MADCAM1* was higher in samples from patients with IBD compared with healthy controls [Figure 1D]. This was positively correlated with clinical disease activity in UC and with endoscopic disease activity in CD [Figure 1E]. Moreover, *MADCAM1* levels correlated with tumour necrosis factor [TNF] expression, which had been demonstrated to regulate *MADCAM1* expression,^{22,23} and with the expression of other pro-inflammatory cytokines and cell adhesion molecules such as *VCAM1* and *ICAM1* [Figure 1F] Supplementary Figure 1].

To corroborate increased MAdCAM-1 expression in active IBD at the protein level, we stained sections from the colon of patients with IBD and healthy controls for MAdCAM-1 by immunofluorescence. We observed substantially higher numbers of MAdCAM-1⁺ cells in the lamina propria of patients with UC and CD compared with controls [Figure 1G].

Finally, since several alternatively spliced transcripts of *MADCAM1* have been described,²⁴ we used the above-mentioned RNA-seq data to interrogate which transcripts are expressed in the gut of patients with IBD. ENST00000215637.8, which encodes a ‘full’ MAdCAM-1 protein with three IgG domains and a mucin-like domain,²⁴ was the transcript variant almost exclusively expressed and this did not differ between inactive and active disease or between CD and UC. [Figure 1H].

Together, these data indicated that increased MAdCAM-1 expression in active IBD contributes to the important role of immune cell trafficking and corroborated that MAdCAM-1 is an interesting candidate target for the therapy of IBD.⁷

3.2. Ontamalimab leads to internalization of MAdCAM-1

Thus, we aimed to understand how the anti-MAdCAM-1 antibody ontamalimab acts on a cellular level. To this end, we overexpressed MAdCAM-1 on HEK293T cells and incubated them with fluorescently labelled ontamalimab. 2D, 3D and time-lapse fluorescence and/or confocal microscopy consistently demonstrated that after binding to MAdCAM-1 on the cell membrane, ontamalimab translocates to the cytosol and particularly into lysosomes [Figure 2; Supplementary

Figure 2 and Video]. This suggested that the ontamalimab–MAdCAM-1 complex is internalized similar to what has been shown for vedolizumab or etrolizumab.^{25,26} Moreover, these data indicated that ontamalimab might not only block the interaction of $\alpha 4\beta 7$ with MAdCAM-1 via the actual target of ontamalimab in the D1 domain,⁸ but that ontamalimab-induced internalization of MAdCAM-1 might also hinder the interaction of L-selectin with MAdCAM-1 via the distant mucin-like domain.¹⁰

3.3. Ontamalimab but not vedolizumab blocks the rolling of adaptive and innate immune cells from IBD patients on MAdCAM-1

Therefore, we sought to clarify the effects of ontamalimab on the rolling and adhesion of immune cells in comparison to vedolizumab, which, as an anti- $\alpha 4\beta 7$ integrin antibody, does not interfere with L-selectin–MAdCAM-1 interactions. In a first series of experiments, we explored the dynamic adhesion of CD4⁺ T cells, CD8⁺ T cells and naïve CD4⁺ T cells from the peripheral blood of patients with and without IBD to MAdCAM-1 using a previously established assay.²⁷ As expected, we observed that both vedolizumab and ontamalimab clearly blocked the adhesion of T cells to MAdCAM-1. The effects of the two antibodies were similar and did not differ between disease entities or the different cell subsets [Supplementary Figure 3A–C].

Next, we employed a rolling assay, in which we perfused fluorescently labelled cells through a ‘flow chamber’ and monitored cell movements by time-lapse confocal microscopy. By software-based analysis of sequential images, we determined the moving speed of the cells in the chamber [Figure 3A and B]. Rolling cells were defined as moving at <30 $\mu\text{m/s}$.²⁸ While treatment with vedolizumab did not affect the rolling of peripheral blood CD4⁺ T cells, ontamalimab clearly reduced the fraction of rolling cells. Again, this was similar in IBD and non-IBD patients [Figure 3C] and also the case in naïve CD4⁺ T cells [Supplementary Figure 3D]. Moreover, ontamalimab also blocked the rolling of CD4⁺ T cells from IBD patients treated with vedolizumab or infliximab in the clinic in a similar fashion, further demonstrating that this effect differentiates vedolizumab and ontamalimab [Supplementary Figure 3E].

Importantly, the effects of ontamalimab were comparable to anti-CD62L treatment, and anti-CD62L treatment in combination with ontamalimab did not have additive effects. Moreover, ontamalimab did not affect the rolling on VCAM-1, whereas anti-CD62L did [Figure 3D]. Thus, these data were consistent with a MAdCAM-1-specific inhibition of L-selectin-dependent CD4⁺ T cell rolling by ontamalimab.

Since L-selectin is not only expressed on T cells, but also on innate immune cells such as granulocytes and monocytes [Supplementary Figure 4], we wondered whether ontamalimab might also interfere with rolling of these cells. Indeed, we observed substantially reduced rolling of granulocytes and monocytes isolated from the peripheral blood upon treatment with ontamalimab, but not vedolizumab [Figure 3E].

or UC as indicated upon perfusion through MAdCAM-1-coated flow chambers and treatment with and without ontamalimab or vedolizumab. [D] Fraction of rolling CD4⁺ T cells perfused through flow chambers coated with MAdCAM-1 [left panel] or VCAM-1 [right panel] and treated with and without anti-CD62L and/or ontamalimab or vedolizumab. [E] Left panels: representative time-lapse microscopy demonstrating rolling [red] and not rolling [white] granulocytes and monocytes during perfusion through MAdCAM-1-coated flow chambers. Right panels: fraction of rolling granulocytes and monocytes upon perfusion through MAdCAM-1-coated flow chambers and treatment with or without ontamalimab or vedolizumab. * $p < 0.05$, ** $p < 0.01$, *** $p < 0.001$ [for all comparisons or the comparisons indicated by line], $n = 5$ for each bar plot.

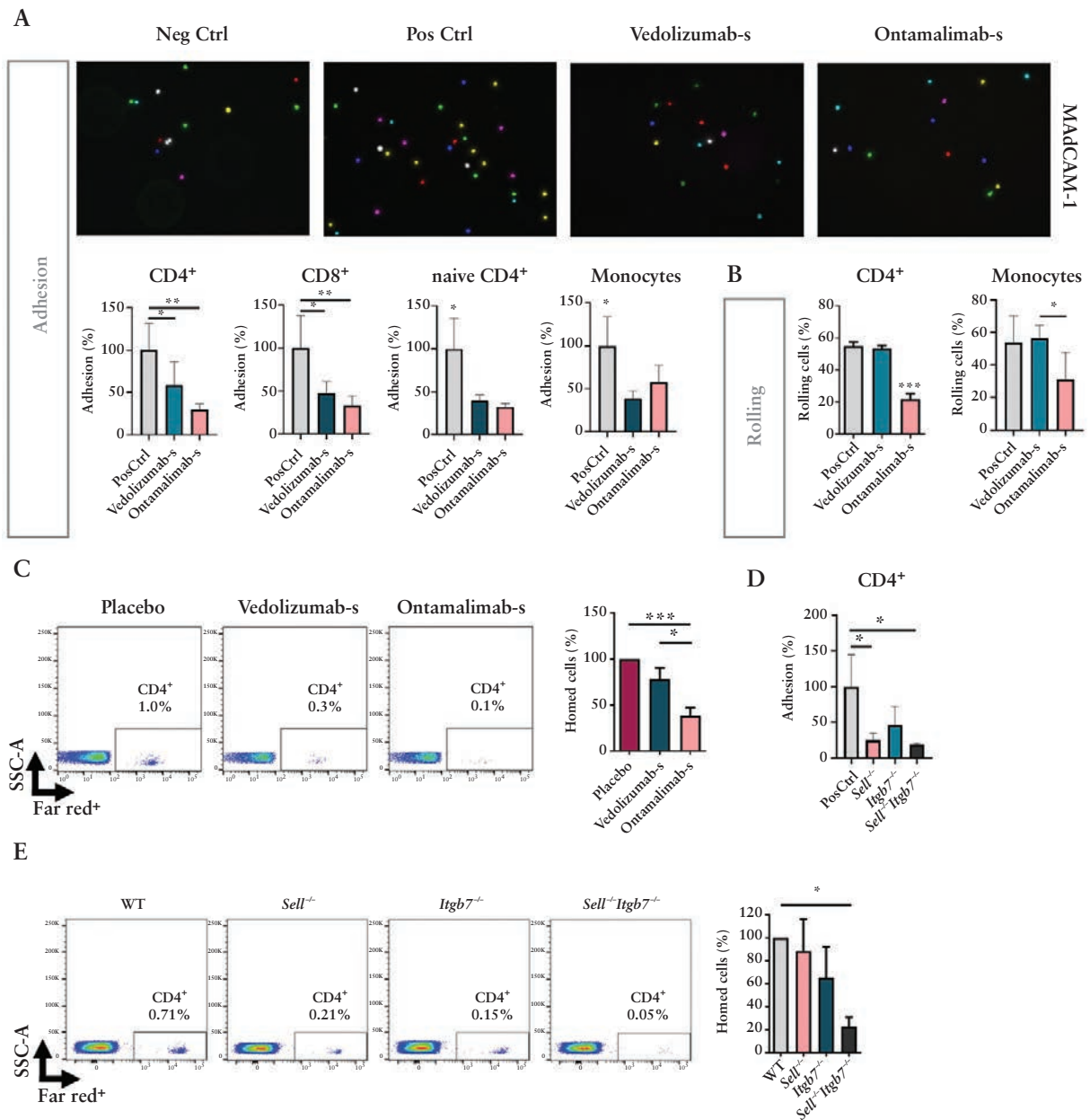


Figure 4. Improved blockade of *in vivo* gut homing with anti-MAdCAM-1 vs. anti- $\alpha 4\beta 7$. [A] Dynamic adhesion assays with different T cell subsets from the spleen and monocytes from the bone marrow of C57BL/6J mice in capillaries coated with MAdCAM-1. Cells were treated with or without anti- $\alpha 4\beta 7$ integrin [vedolizumab-s] or anti-MAdCAM-1 antibodies [ontamalimab-s] [$n = 5$ for each cell type]. Upper panels: representative fluorescence microscopy. Lower panels: quantification of adhering cells relative to the average of the positive control. [B] Fraction of rolling CD4⁺ T cells and monocytes on MAdCAM-1 upon treatment with or without vedolizumab-s or ontamalimab-s [$n = 5-9$ per group]. [C] *In vivo* homing of CD4⁺ splenocytes from C57BL/6J mice labelled with CellTrace FarRed and transferred to *Rag1*^{-/-} recipients upon treatment with vedolizumab-s, ontamalimab-s or placebo [rat IgG]. Left panels: representative flow cytometry of FarRed⁺ cells in the lamina propria after 24 h. Right panel: quantitative flow cytometry indicating the relative frequency of homed FarRed⁺ cells in the lamina propria [$n = 9-11$ per group]. [D] Dynamic adhesion assays with CD4⁺ T cells from C57BL/6J, *Sell*^{-/-}, *Itgb7*^{-/-} and *Sell*^{-/-}*Itgb7*^{-/-} mice in capillaries coated with MAdCAM-1. Quantification of adhering cells relative to the average of the positive control [$n = 3$]. [E] *In vivo* homing of CD4⁺ splenocytes from C57BL/6J, *Sell*^{-/-}, *Itgb7*^{-/-} and *Sell*^{-/-}*Itgb7*^{-/-} mice labelled with CellTrace FarRed and transferred to *Rag1*^{-/-} recipients. Quantitative flow cytometry indicating the relative frequency of homed FarRed⁺ cells in the lamina propria [$n = 3-4$ per group, comparisons with paired *t*-test]. * $p < 0.05$, ** $p < 0.01$, *** $p < 0.001$ [for all comparisons or the comparisons indicated by line].

Together, these results supported the concept that anti-MAdCAM-1, but not anti- $\alpha 4\beta 7$, treatment blocks the rolling of adaptive and innate immune cells on MAdCAM-1.

3.4. Ontamalimab-s is superior to vedolizumab-s in reducing T cell homing *in vivo*

In the next step, we wanted to determine whether these mechanistic differences also lead to altered homing to the

gut *in vivo*. Since the expression of $\alpha 4\beta 7$ and MAdCAM-1 on circulating immune cells and the intestinal endothelium, respectively, prohibited us from addressing this question in previously established humanized mouse models,²⁹ we chose a fully murine system. Accordingly, we used the surrogate antibodies DATK32 [vedolizumab-s] and MECA367 [ontamalimab-s] and initially confirmed in *in vitro* adhesion and rolling assays with T cells and monocytes that the

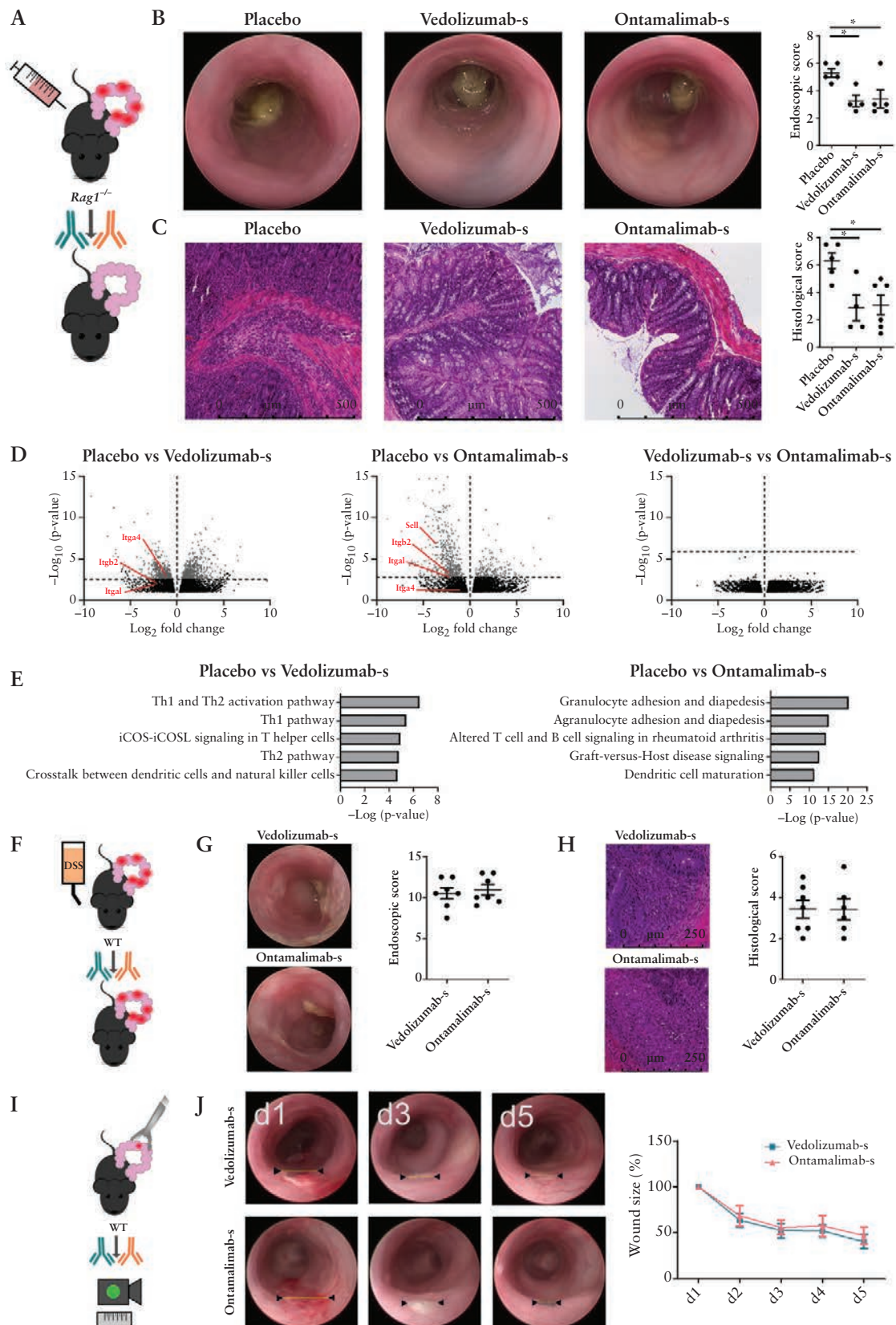


Figure 5. Similar effects of ontamalimab-s and vedolizumab-s in experimental models of colitis and wound healing. [A–E] T cell transfer colitis in *Rag1*^{-/-} mice treated with vedolizumab-s, ontamalimab-s or placebo after transfer of naive CD4⁺ splenocytes from C57BL/6J mice. [A] Schematic depiction of the experiment. [B] Representative colonoscopy at day 42 [left panels] and scoring of endoscopic disease activity [right panel, $n = 4$ –5 per group]. [C] Representative H/E staining of colon tissue at day 42 [left panels] and histological scoring of disease activity [right panel, $n = 4$ –6 per group]. [D] Volcano plots comparing gene expression in inflamed colon tissue as determined by RNA sequencing between vedolizumab-s-, ontamalimab-s- and placebo-treated mice and highlighting selected genes involved in cell trafficking pathways. The dashed horizontal line marks significance level [adjusted $p \leq 0.05$]. [E] Ingenuity pathway analysis of RNA sequencing results showing the top five regulated pathways in vedolizumab-s- or ontamalimab-s-treated mice

differential mechanisms of anti-MAdCAM-1 and anti- $\alpha 4\beta 7$ blockade are conserved between species [Figure 4A and B]. When transferring CD4⁺ splenocytes to *Rag1*^{-/-} mice *in vivo* and treating them with vedolizumab-s or ontamalimab-s, the reduction of T cell infiltration to the gut was even more pronounced by ontamalimab-s compared with vedolizumab-s [Figure 4C].

We also used mice deficient for L-selectin [*Sell*] and/or integrin $\beta 7$ [*Itgb7*] to confirm these findings. Both knockouts as well as the combination led to reduced dynamic adhesion of CD4⁺ T cells from the spleen to MAdCAM-1 [Figure 4D]. While *Sell* deficiency alone had no effect *in vivo*, *Itgb7* deficiency and even more the combination of *Itgb7* and *Sell* deficiency reduced the gut homing of these cells [Figure 4E], indicating that the combined blockade of rolling and adhesion is more effective than adhesion alone.

Collectively, these data suggested that ontamalimab-s also has a broader mechanism of action on T cell trafficking *in vivo*.

3.5. Comparable effects of ontamalimab-s and vedolizumab-s across multiple experimental models

Thus, we wondered whether this also translates into differential effects of ontamalimab-s and vedolizumab-s in experimental models of colitis. To this end, we transferred naïve CD4⁺ T cells from the spleen of wild-type mice to *Rag1*^{-/-} mice to induce T cell transfer colitis and treated the mice with ontamalimab-s, vedolizumab-s or placebo [Figure 5A]. Both treatments alleviated disease severity as assessed by endoscopy and histology on day 42 [Figure 5B and C]. However, there was no difference in disease severity between ontamalimab-s- and vedolizumab-s-treated mice. To explore the mechanisms behind these similar outcomes, we performed bulk RNA-seq of colon tissue from those mice. Interestingly, although—in accordance with the similar phenotype—only a few genes were differentially regulated between ontamalimab-s- and vedolizumab-s-treated mice, differential gene regulation was observed compared with placebo-treated mice. Indeed, some key cell trafficking genes such as integrin $\alpha 4$ [*Itga4*] were regulated only in the vedolizumab-s-treated group, while integrin αL [*Itgal*], integrin $\beta 2$ [*Itgb2*] and *Sell* were only regulated in the ontamalimab-s-treated group [Figure 5D]. Consistently, IPA of regulated canonical pathways showed differential pathway activation. While, compared to placebo-treated mice, pathways associated with T helper [Th]1 and Th2 cells were predominantly affected in vedolizumab-s-treated mice, cell trafficking pathways ranked highest in ontamalimab-s-treated mice [Figure 5E]. Thus, these data indicated differential mechanisms of ontamalimab-s and vedolizumab-s on a molecular level but with similar phenotypic effects.

Since we had shown above that ontamalimab also acts on innate immune cell subsets, we further compared anti-MAdCAM-1 versus anti- $\alpha 4\beta 7$ blockade in DSS colitis as a

model, which is predominantly dependent on innate immunity [Figure 5F].³⁰ However, there was no difference in endoscopic and histological disease activity between wild-type mice treated with ontamalimab-s or vedolizumab-s [Figure 5G and H].

Finally, as we have previously shown that innate immune cell trafficking also impacts on intestinal wound healing,³¹ we compared the effects of ontamalimab-s and vedolizumab-s on the healing of mucosal defects inflicted with a biopsy forceps [Figure 5I]. Again, we did not observe differences [Figure 5J].

Taken together, these data suggested that anti-MAdCAM-1 and anti- $\alpha 4\beta 7$ treatment do not differ in their overall effects in experimental models of colitis and wound healing, although different mechanisms are involved.

3.6. Alternative mechanisms are functional in CD8⁺T cells to evade effects of anti-MAdCAM-1 antibodies

We therefore wondered how this discrepancy between *in vitro* and *in vivo* findings can be resolved. Accordingly, we performed single-cell RNA-seq of LPMCs from DSS-treated wild-type mice treated with ontamalimab-s, vedolizumab-s or placebo.

To focus on leukocytes, we selected cells expressing *Ptpnc* [Supplementary Figure 5A]. Within these cells, we identified 14 clusters [Figure 6A]. Interestingly, when we compared the expression of genes centrally involved in gut homing such as *Itga4*, *Itgb7* or C-C chemokine receptor 9 [*Ccr9*] between those clusters, we observed striking differences [Figure 6B], suggesting that different cell trafficking pathways guide the recruitment of cells in these subsets. Thus, we compared the proportion of cells from vedolizumab-s-, ontamalimab-s- and placebo-treated mice that were present in each cluster [Figure 6C] and observed profound differences: substantially fewer cells from mice treated with vedolizumab-s and ontamalimab-s were present in cluster 6, which was enriched for cells expressing *Cd19* [Figure 6D] and therefore most likely comprised B cells. This indicated that blockade of $\alpha 4\beta 7$ -MAdCAM-1 interactions inhibited the recruitment of B cells to the lamina propria. By contrast, there was a clear enrichment of ontamalimab-s-treated cells in clusters 4 and 7 [Figure 6C], suggesting that these cells may home to the gut despite the presence of ontamalimab-s. As indicated by the expression of *Ly6g* and *Cd3d* [Figure 6D], these clusters probably comprised granulocytes and T cells, respectively. Moreover, further expression analysis indicated that numerous genes associated with cytotoxicity including *Gzmb*, *Gzma* or *Prf1* are specifically expressed in cluster 7, suggesting that substantial accumulation of cytotoxic T cells and other cytotoxic cells occurs under treatment with ontamalimab-s [Figure 6E; Supplementary Figure 5B]. Importantly, we did not find a similar enrichment in the relative abundance of cells from anti-MAdCAM-1-treated mice in the CD4⁺ T cell subpopulations located in subclusters of cluster 2 [Supplementary Figure 5C]. This was corroborated

compared to placebo-treated mice. [F–H] DSS-induced colitis in C57BL/6J mice treated with vedolizumab-s or ontamalimab-s. [F] Schematic depiction of the experiment. [G] Representative colonoscopy at day 10 [left panels] and scoring of endoscopic disease activity [right panel, $n = 7$ per group]. [H] Representative H/E staining of colon tissue at day 10 [left panels] and histological scoring of disease activity [right panel, $n = 6$ –8 per group]. [I–J] Tracking of colon wound healing in C57BL/6J mice upon treatment with vedolizumab-s or ontamalimab-s. [I] Schematic depiction of the experiment. [J] Left panels: representative endoscopy of wounds on days 1, 3 and 5. Black arrowheads indicate the outer wound edges. Right panels: time course of wound closure. Diameters of each wound are normalized to the respective wound diameter on day 1 [$n = 6$ per group]. DSS, dextran sodium sulphate. * $p < 0.05$, ** $p < 0.01$, *** $p < 0.001$.

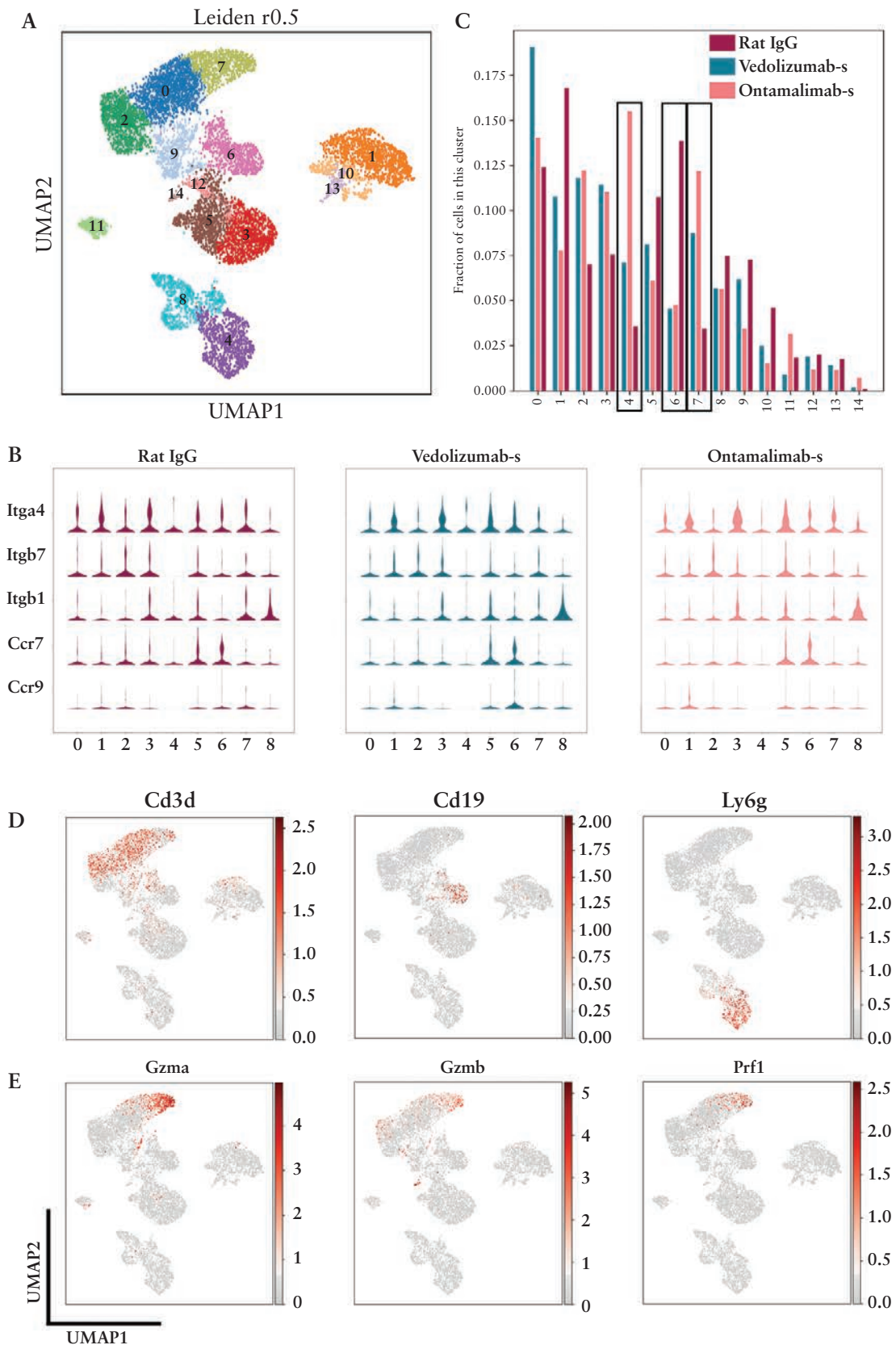


Figure 6. Single cell RNA sequencing reveals heterogeneous impact on ontamalimab-s on specific immune cell subsets. DSS colitis was induced in C57BL/6J mice and mice were treated with vedolizumab-s, ontamalimab-s or placebo. Single cell RNA sequencing was performed on CD45⁺ lamina propria mononuclear cells isolated on day 10. Cells from two mice were pooled per treatment group. [A] UMAP plot of *Pctrcp*-enriched cells [see [Supplementary Figure 5A](#)] showing 14 clusters generated based on the Leiden algorithm at resolution 0.5. [B] Proportion of cells from each treatment group per cluster. Clusters 4 and 7, where ontamalimab-s-treated cells are relatively enriched, as well as cluster 6, where ontamalimab-s- and vedolizumab-s-treated cells are reduced, are highlighted. [C] Violin plots displaying the expression of selected genes associated with cell trafficking pathways in clusters 0–8. [D] UMAP plots displaying the expression of *Cd3d*, *Cd19*, *Ly6g*, *Gzma*, *Gzmb* and *Prf1*.

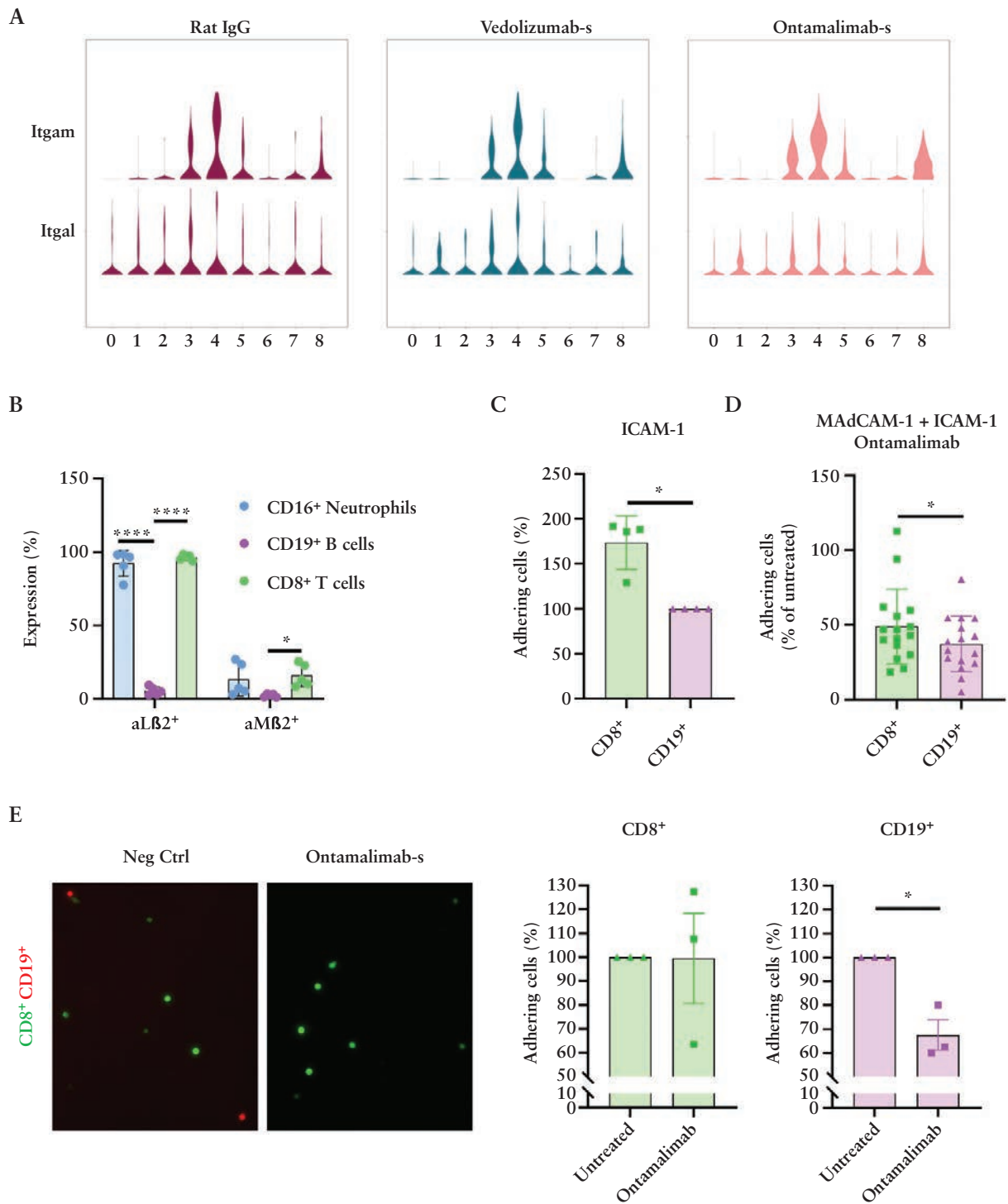


Figure 7. Alternative cell trafficking pathways are active in ontamalimab-treated CD8⁺ T cells. [A] Violin plots displaying the expression of *Itgal* and *Itgam* in clusters 0–8 from the single cell RNA sequencing presented in Figure 6. [A] Quantitative flow cytometry of α Lβ2 and α Mβ2 expression on human peripheral blood CD3⁺CD8⁺ T cells, CD66b⁺CD16⁻ neutrophils and CD3⁻CD19⁺ B cells [*n* = 5]. [C] Quantitative dynamic adhesion of CD8⁺ T cells and CD19⁺ B cells from the peripheral human blood in capillaries coated with ICAM-1 [*n* = 4]. [D] Quantitative dynamic adhesion of CD8⁺ T cells and CD19⁺ B cells from the peripheral human blood treated with ontamalimab to capillaries coated with ICAM-1 and MAdCAM-1 [*n* = 16]. Adhesion is expressed as the fraction of adhering untreated cells from the same donor. [E] Representative images [left] and quantification [right] of dynamic adhesion of CD8⁺ T cells (green) and CD19⁺ B cells (red) from the peripheral human blood and treated with or without ontamalimab to IL-1β-activated HUVECs [*n* = 3]. **p* < 0.05.

by flow cytometry demonstrating that the expression of CD4⁺ T cell subset transcription factors such as T-bet, Ror-γt, Gata3 or Foxp3 was similar in mice treated with anti-α4β7 or anti-MAdCAM-1 antibodies [Supplementary Figure 5D].

Thus, we wondered whether alternative gut homing mechanisms not affected by ontamalimab-s might guide CD8⁺ T cells to the gut, while being absent in CD19⁺ B cells. Indeed, cells from cluster 6 expressed almost no *Itgal* and *Itgam*,

whereas some expression could be noted in cluster 7 [Figure 7A]. Even more impressively, human CD8⁺ T cells expressed substantially more α L β 2 and α M β 2 integrins on their surface compared to B cells and had comparable expression to neutrophils [Figure 7B]. Since these integrins functionally interact with ICAM-1, we explored the dynamic adhesion of human CD8⁺ T cells and CD19⁺ B cells to ICAM-1. In line with these expression data, more CD8⁺ T cells than CD19⁺ B cells adhered to ICAM-1 [Figure 7C]. Since ICAM-1 is also expressed on the endothelium in the gut,³² we used additional assays, in which we co-coated MAdCAM-1 together with ICAM-1 and compared the adhesion of ontamalimab-treated CD8⁺ T cells and CD19⁺ B cells. Indeed, a higher fraction [compared to untreated] of the former than of the latter was still able to adhere [Figure 7D]. To come closer to the even more complex situation in the human gut, we used activated human umbilical vein endothelial cells [HUVECs]³³ in a flow-pump system. When we added CD8⁺ T or CD19⁺ B cells and treated them with or without ontamalimab, we observed a significant reduction of adhesion for CD19⁺ B cells, but not for CD8⁺ T cells [Figure 7E].

These findings indicated that while B cells seem to depend substantially on MAdCAM-1-dependent gut homing, this might be accomplished via MAdCAM-1-independent pathways by CD8⁺ T cells co-expressing integrins such as α L β 2. Collectively, these data supported the concept that redundant cell trafficking pathways in specific immune cell populations can override the unique molecular effects of anti-MAdCAM-1 compared with anti- α 4 β 7 antibodies resulting in similar pre-clinical efficacy.

4. Discussion

While many of the therapeutic concepts available for the treatment of IBD such as anti-TNF antibodies, anti-IL-12/23 antibodies of Jak inhibitors had previously already been used in rheumatic or skin diseases,³⁴ anti-trafficking agents have only been approved for multiple sclerosis³⁵ and IBD,³⁻⁵ and IBD is currently the leading field with regard to the development of anti-trafficking agents.²

Since successful pivotal trials with vedolizumab were the break-through for anti-trafficking agents in IBD in 2013,^{3,4} many new substances and antibodies have been designed and investigated for therapeutic use in IBD.³⁶ Many of these approaches centre around gut-specific mechanisms of cell trafficking, including the interaction of MAdCAM-1 and α 4 β 7 integrin.^{9,12,37}

One of these strategies is the anti-MAdCAM-1 antibody ontamalimab. While the mechanisms of vedolizumab have been extensively investigated in recent years,³⁸⁻⁴¹ not much is known about the particular mechanism of action of ontamalimab. Moreover, the prevailing view is that the mechanism of action of ontamalimab should be very similar to that of vedolizumab,^{7,18} but this has not specifically explored to date.

We therefore aimed to address the mechanism of action of ontamalimab and to compare it to vedolizumab. Our data show that ontamalimab must not be understood as a copy of vedolizumab with a different target, since it has a unique and even broader mechanism of action. Specifically, ontamalimab blocked MAdCAM-1-dependent rolling in addition to adhesion and this also applied to innate immune cell subsets. Although vedolizumab has also been shown to interfere with

innate immune cell trafficking,^{31,39} a predominant effect on lymphocytes is still assumed.⁴² Since innate immune cells such as macrophages and granulocytes play a central role in the pathogenesis and the inflammatory network of IBD,^{43,44} these data could therefore suggest improved clinical efficacy compared with vedolizumab. However, this is in contrast to findings in clinical trials^{14,15} that did not come to similar conclusions and also to observations we made in experimental *in vivo* models of IBD and wound healing, where surrogate antibodies were equally effective.

Our data suggest that these similar effects despite different molecular mechanisms are due to redundant pathways permitting gut homing of specific immune cell subsets despite the blockade of MAdCAM-1-dependent rolling. Indeed, several such pathways are conceivable. For example, rolling of immune cells along the vessel wall can also occur via the interaction of α L β 2 with ICAM-1⁴⁵ and α 4 β 1 with VCAM-1,⁴⁶ as well as E- and P-selectin with their respective ligands.⁴⁷⁻⁴⁹ Since these molecules are known to be expressed on high endothelial venules of the gut and on immune cells vitally involved in IBD pathogenesis such as granulocytes and monocytes,⁵⁰ respectively, such evasion of ontamalimab blockade is highly plausible and might also help to maintain mucosal infection control by innate immune cells. Interestingly, given the clinical effects of vedolizumab, which specifically blocks the α 4 β 7-dependent adhesion to MAdCAM-1, these redundancies seem to be particularly relevant at the rolling stage, since abrogated firm adhesion via α 4 β 7 cannot completely be compensated for by other pathways, at least not in all patients. However, these redundant cell trafficking pathways can, in principle, also mitigate the effects of vedolizumab, as previously demonstrated.⁵¹

There is also another potential explanation to be considered for the comparable effects of vedolizumab-s and ontamalimab-s in experimental models: pro- and anti-inflammatory immune cell subsets share gut homing pathways.¹ We have recently shown that vedolizumab, but not the anti- β 7 antibody etrolizumab-s, differentially targets regulatory and effector T cells in a certain concentration range, leading to residual gut homing of highly suppressive regulatory T cells in parallel to broadly blocked effector T cell recruitment.^{52,53} While this seems to contribute to the clinical efficacy of vedolizumab, things may be different with ontamalimab. Thus, it is not easy to predict what the blockade of a specific pathway means for the balance of diverse subsets with context-sensitive pro- or anti-inflammatory functions and how this eventually reflects in clinical phenotypes.

In a translational perspective, the key question is what our data imply for clinical management of patients with IBD. In this regard, a limitation of our study is that we did not have access to samples from patients treated with ontamalimab. However, on the one hand, our findings underline that cell trafficking pathways are complex and that the pure consideration of antibody binding sites and ligands falls short of precisely predicting mechanisms and efficacy of an approach. Thus, detailed mechanistic investigations are necessary to understand the effects of current and future anti-trafficking strategies. Moreover, these complex pathways need to be considered when envisioning personalized treatment strategies, since the mechanisms might differ between individuals. On the other hand, our data justify and substantiate anti-MAdCAM-1 as an independent approach for IBD therapy and indicate that it might have similar potential to

vedolizumab. Along these lines, our findings will be of key importance for the interpretation of pending data from the ontamalimab phase III trials, which were terminated at an early stage after a company takeover and will therefore not be sufficient to prove efficacy and safety. They will, however, inform whether ontamalimab has sufficient efficacy to warrant further development as a treatment for patients with IBD.

In conclusion, our data are the first to demonstrate a unique and broader mechanism of action of ontamalimab compared to vedolizumab, while they also indicate that this extended mechanism is compensated for by alternative cell trafficking pathways and the efficacy in preclinical models is comparable. Thus, they offer explanations for past and future questions arising from clinical trials with ontamalimab.

Funding

This work was supported through a grant by Shire, a Takeda company. The company had no role in experimental design, analysis or interpretation of the results. This work was further supported by the Deutsche Forschungsgemeinschaft [DFG, German Research Foundation; ZU 377/4-1, STU 238/10-1, TRR 241 – 375876048, projects A06, B01, B08, C04, Z03] and the Else Kröner-Fresenius-Stiftung [2021_EKCS.23] as well as the Corona-funding initiative of the Bavarian Ministry of Science and Arts to MS.

Conflict of Interest

M.F.N. has served as an advisor for Pentax, Giuliani, MSD, Abbvie, Janssen, Takeda and Boehringer. S.Z. received speaker's fees from Takeda, Roche, Galapagos, Ferring, Lilly, Falk and Janssen. M.F.N. and S.Z. received research support from Takeda, Shire [a part of Takeda] and Roche. D.P. and D. S. are employees of Takeda and own stock and/or stock options in Takeda. B.S. has served as consultant for Abbvie, Arena, BMS, Boehringer, Celgene, Falk, Galapagos, Janssen, Lilly, Pfizer, Prometheus and Takeda and received speaker's fees from Abbvie, CED Service GmbH, Falk, Ferring, Janssen, Novartis, Pfizer and Takeda [served as representative of the Charité]. The other authors declare no conflicts of interest.

Acknowledgments

The research of T.M.M., I.A., M.S., M.L., R.A., M.F.N. and S.Z. was supported by the Interdisciplinary Center for Clinical Research [IZKF] and the ELAN programme of the Universität Erlangen-Nürnberg, the Fritz-Bender-Stiftung, the Ernst Jung-Stiftung, the Else Kröner-Fresenius-Stiftung, the Thyssen-Stiftung, the German Crohn's and Colitis Foundation [DCCV], the DFG topic programme on Microbiota, the Emerging Field Initiative, the DFG Collaborative Research Centers 643, 796, 1181 and TRR241 [Project-ID 375876048—TRR 241], the Rainin Foundation and the Litwin IBD Pioneers programme of the Crohn's and Colitis Foundation of America [CCFA]. The authors thank J. Derdau, D. Dziony, J. Marcks and J. Schuster for their invaluable technical assistance. Further thanks go to Dr Helen Kühn, Dr Anja Schulz-Kuhnt and Dr Julia Krug for support of method establishment, experimental design and evaluation. We thank Prof. Andreas Kremer for providing HEK293T cells.

Author Contributions

L.L.S., E.B., L.L., C.vP., M.M.A. and T.M.M. performed the experiments. L.L.S., M.F.N. and S.Z. designed the study and analysed and interpreted the data. M.D., A.B.E. and P.K. analysed transcriptomic data. E.B., M.W., K.A.U., T.M.M., I.A., M.L., M.S., R.A., B.S., TRR241, M.F.N. and S.Z. provided clinical samples, protocols or reagents; L.L.S. and S.Z. drafted the manuscript; all authors critically revised the manuscript for important intellectual content.

Data Availability

Data are available from the authors upon reasonable request. Transcriptomic data are deposited at NCBI under PRJNA980589 and GSE230059.

Supplementary Data

Supplementary data are available at ECCO-JCC online.

References

- Habtezion A, Nguyen LP, Hadeiba H, Butcher EC. Leukocyte trafficking to the small intestine and colon. *Gastroenterology* 2016;150:340–54. doi:10.1053/j.gastro.2015.10.046.
- Zundler S, Becker E, Schulze LL, Neurath MF. Immune cell trafficking and retention in inflammatory bowel disease: mechanistic insights and therapeutic advances. *Gut* 2019;68:1688–700. doi:10.1136/gutjnl-2018-317977.
- Feagan BG, Rutgeerts P, Sands BE, et al; GEMINI 1 Study Group. Vedolizumab as induction and maintenance therapy for ulcerative colitis. *N Engl J Med* 2013;369:699–710. doi:10.1056/NEJMoa1215734.
- Sandborn WJ, Feagan BG, Rutgeerts P, et al; GEMINI 2 Study Group. Vedolizumab as induction and maintenance therapy for Crohn's disease. *N Engl J Med* 2013;369:711–21. doi:10.1056/NEJMoa1215739.
- Sandborn WJ, Feagan BG, D'Haens G, et al. Ozanimod as induction and maintenance therapy for ulcerative colitis. *N Engl J Med* 2021;385:1280–91. doi:10.1056/NEJMoa2033617.
- Zundler S, Günther C, Kremer AE, Zaiss MM, Rothhammer V, Neurath MF. Gut immune cell trafficking: inter-organ communication and immune-mediated inflammation. *Nat Rev Gastroenterol Hepatol* 2023;20:50–64. doi:10.1038/s41575-022-00663-1.
- Duijvestein M, D'Haens GR. Rational and clinical development of the anti-MAdCAM monoclonal antibody for the treatment of IBD. *Expert Opin Biol Ther* 2019;19:361–6. doi:10.1080/14712598.2019.1576631.
- Yu Y, Zhu J, Huang P-S, Wang J-H, Pullen N, Springer TA. Domain 1 of mucosal addressin cell adhesion molecule has an I1-set fold and a flexible integrin-binding loop. *J Biol Chem* 2013;288:6284–94. doi:10.1074/jbc.M112.413153.
- Briskin M, Winsor-Hines D, Shyjan A, et al. Human mucosal addressin cell adhesion molecule-1 is preferentially expressed in intestinal tract and associated lymphoid tissue. *Am J Pathol* 1997;151:97–110.
- Berg EL, McEvoy LM, Berlin C, Bargatze RF, Butcher EC. L-selectin-mediated lymphocyte rolling on MAdCAM-1. *Nature* 1993;366:695–8. doi:10.1038/366695a0.
- Sun H, Liu J, Zheng Y, Pan Y, Zhang K, Chen J. Distinct chemokine signaling regulates integrin ligand specificity to dictate tissue-specific lymphocyte homing. *Dev Cell* 2014;30:61–70. doi:10.1016/j.devcel.2014.05.002.
- Berlin C, Berg EL, Briskin MJ, et al. $\alpha 4\beta 7$ integrin mediates lymphocyte binding to the mucosal vascular addressin MAdCAM-1. *Cell* 1993;74:185–95. doi:10.1016/0092-8674(93)90305-A.

13. Dotan I, Allez M, Danese S, Keir M, Tole S, McBride J. The role of integrins in the pathogenesis of inflammatory bowel disease: Approved and investigational anti-integrin therapies. *Med Res Rev* 2020;40:245–62. doi:10.1002/med.21601.
14. Vermeire S, Sandborn WJ, Danese S, et al. Anti-MAdCAM antibody (PF-00547659) for ulcerative colitis (TURANDOT): a phase 2, randomised, double-blind, placebo-controlled trial. *Lancet* 2017;390:135–44. doi:10.1016/S0140-6736(17)30930-3.
15. Sandborn WJ, Lee SD, Tarabar D, et al. Phase II evaluation of anti-MAdCAM antibody PF-00547659 in the treatment of Crohn's disease: report of the OPERA study. *Gut* 2018;67:1824–35. doi:10.1136/gutjnl-2016-313457.
16. Schreiner P, Neurath MF, Ng SC, et al. Mechanism-based treatment strategies for IBD: cytokines, cell adhesion molecules, Jak inhibitors, gut flora, and more. *Inflamm Intest Dis* 2019;4:79–96. doi:10.1159/000500721.
17. Pérez-Jeldres T, Tyler CJ, Boyer JD, et al. Cell trafficking interference in inflammatory bowel disease: therapeutic interventions based on basic pathogenesis concepts. *Inflamm Bowel Dis* 2019;25:270–82. doi:10.1093/ibd/izy269.
18. Allocca M, Fiorino G, Vermeire S, Reinisch W, Cataldi F, Danese S. Blockade of lymphocyte trafficking in inflammatory bowel diseases therapy: importance of specificity of endothelial target. *Expert Rev Clin Immunol* 2014;10:885–95. doi:10.1586/1744666X.2014.917962.
19. Soler D, Chapman T, Yang L-L, Wyant T, Egan R, Fedyk ER. The binding specificity and selective antagonism of vedolizumab, an anti- α 4 β 7 integrin therapeutic antibody in development for inflammatory bowel diseases. *J Pharmacol Exp Ther* 2009;330:864–75. doi:10.1124/jpet.109.153973.
20. Arihiro S, Ohtani H, Suzuki M, et al. Differential expression of mucosal addressin cell adhesion molecule-1 (MAdCAM-1) in ulcerative colitis and Crohn's disease. *Pathol Int* 2002;52:367–74. doi:10.1046/j.1440-1827.2002.01365.x.
21. Keir ME, Fuh F, Ichikawa R, et al. Regulation and role of α E integrin and gut homing integrins in migration and retention of intestinal lymphocytes during inflammatory bowel disease. *J Immunol* 2021;207:2245–54. doi:10.4049/jimmunol.2100220.
22. Ogawa H, Binion DG, Heidemann J, et al. Mechanisms of MAdCAM-1 gene expression in human intestinal microvascular endothelial cells. *Am J Physiol Cell Physiol* 2005;288:C272–81. doi:10.1152/ajpcell.00406.2003.
23. Ando T, Langley RR, Wang Y, et al. Inflammatory cytokines induce MAdCAM-1 in murine hepatic endothelial cells and mediate α 4 β 7 integrin dependent lymphocyte endothelial adhesion in vitro. *BMC Physiol* 2007;7:10. doi:10.1186/1472-6793-7-10.
24. Sampaio SO, Li X, Takeuchi M, et al. Organization, regulatory sequences, and alternatively spliced transcripts of the mucosal addressin cell adhesion molecule-1 (MAdCAM-1) gene. *J Immunol* 1995;155:2477–86.
25. Wyant T, Yang L, Fedyk E. In vitro assessment of the effects of vedolizumab binding on peripheral blood lymphocytes. *MAbs* 2013;5:842–50. doi:10.4161/mabs.26392.
26. Lichnog C, Klabunde S, Becker E, et al. Cellular mechanisms of etrolizumab treatment in inflammatory bowel disease. *Front Pharmacol* 2019;10:39. doi:10.3389/fphar.2019.00039.
27. Binder M-T, Becker E, Wiendl M, et al. Similar inhibition of dynamic adhesion of lymphocytes from IBD patients to MAdCAM-1 by vedolizumab and etrolizumab-s. *Inflamm Bowel Dis* 2018;24:1237–50. doi:10.1093/ibd/izy077.
28. Rijcken E, Mennigen RB, Schaefer SD, et al. PECAM-1 (CD 31) mediates transendothelial leukocyte migration in experimental colitis. *Am J Physiol Gastrointest Liver Physiol* 2007;293:G446–52. doi:10.1152/ajpgi.00097.2007.
29. Zundler S, Schillinger D, Fischer A, et al. Blockade of α E β 7 integrin suppresses accumulation of CD8⁺ and Th9 lymphocytes from patients with IBD in the inflamed gut in vivo. *Gut* 2017;66:1936–48. doi:10.1136/gutjnl-2016-312439.
30. Wirtz S, Popp V, Kindermann M, et al. Chemically induced mouse models of acute and chronic intestinal inflammation. *Nat Protoc* 2017;12:1295–309. doi:10.1038/nprot.2017.044.
31. Schleier L, Wiendl M, Heidbreder K, et al. Non-classical monocyte homing to the gut via α 4 β 7 integrin mediates macrophage-dependent intestinal wound healing. *Gut* 2020;69:252–63. doi:10.1136/gutjnl-2018-316772.
32. Reinisch W, Hung K, Hassan-Zahrae M, Cataldi F. Targeting endothelial ligands: ICAM-1/alicaforsen, MAdCAM-1. *J Crohns Colitis* 2018;12:S669–77. doi:10.1093/ecco-jcc/jjy059.
33. Lindholm C, Naylor A, Johansson E-L, Quiding-Järbrink M. Mucosal vaccination increases endothelial expression of mucosal addressin cell adhesion molecule 1 in the human gastrointestinal tract. *Infect Immun* 2004;72:1004–9. doi:10.1128/IAI.72.2.1004-1009.2004.
34. Schett G, McInnes IB, Neurath MF. Reframing immune-mediated inflammatory diseases through signature cytokine hubs. *N Engl J Med* 2021;385:628–39. doi:10.1056/NEJMra1909094.
35. Polman CH, O'Connor PW, Havrdova E, et al; AFFIRM Investigators. A randomized, placebo-controlled trial of natalizumab for relapsing multiple sclerosis. *N Engl J Med* 2006;354:899–910. doi:10.1056/NEJMoa044397.
36. Wiendl M, Becker E, Müller TM, Voskens CJ, Neurath MF, Zundler S. Targeting immune cell trafficking – insights from research models and implications for future IBD therapy. *Front Immunol* 2021;12:656452. doi:10.3389/fimmu.2021.656452.
37. Iwata M, Hirakiyama A, Eshima Y, Kagechika H, Kato C, Song S-Y. Retinoic acid imprints gut-homing specificity on T cells. *Immunity* 2004;21:527–38. doi:10.1016/j.immuni.2004.08.011.
38. Uzzan M, Tokuyama M, Rosenstein AK, et al. Anti- α 4 β 7 therapy targets lymphoid aggregates in the gastrointestinal tract of HIV-1-infected individuals. *Sci Transl Med* 2018;10:eaau4711. doi:10.1126/scitranslmed.aau4711.
39. Zeissig S, Rosati E, Dowds CM, et al. Vedolizumab is associated with changes in innate rather than adaptive immunity in patients with inflammatory bowel disease. *Gut* 2019;68:25–39. doi:10.1136/gutjnl-2018-316023.
40. Fischer A, Zundler S, Atreya R, et al. Differential effects of α 4 β 7 and GPR15 on homing of effector and regulatory T cells from patients with UC to the inflamed gut in vivo. *Gut* 2016;65:1642–64. doi:10.1136/gutjnl-2015-310022.
41. Zundler S, Klingberg A, Schillinger D, et al. Three-dimensional cross-sectional light-sheet microscopy imaging of the inflamed mouse gut. *Gastroenterology* 2017;153:898–900. doi:10.1053/j.gastro.2017.07.022.
42. Neurath MF. Targeting immune cell circuits and trafficking in inflammatory bowel disease. *Nat Immunol* 2019;20:970–9. doi:10.1038/s41590-019-0415-0.
43. Dharmasiri S, Garrido-Martin EM, Harris RJ, et al. Human intestinal macrophages are involved in the pathology of both ulcerative colitis and Crohn disease. *Inflamm Bowel Dis* 2021;27:1641–52. doi:10.1093/ibd/izab029.
44. Fournier BM, Parkos CA. The role of neutrophils during intestinal inflammation. *Mucosal Immunol* 2012;5:354–66. doi:10.1038/mi.2012.24.
45. Zhou F, Zhang F, Zarnitsyna VI, et al. The kinetics of E-selectin- and P-selectin-induced intermediate activation of integrin α L β 2 on neutrophils. *J Cell Sci* 2021;134:jcs.258046. doi:10.1242/jcs.258046.
46. Berlin C, Bargatze RF, Campbell JJ, et al. Alpha 4 integrins mediate lymphocyte attachment and rolling under physiologic flow. *Cell* 1995;80:413–22. doi:10.1016/0092-8674(95)90491-3.
47. Doré M, Korthuis RJ, Granger DN, Entman ML, Smith CW. P-selectin mediates spontaneous leukocyte rolling in vivo. *Blood* 1993;82:1308–16.
48. Yago T, Shao B, Miner JJ, et al. E-selectin engages PSGL-1 and CD44 through a common signaling pathway to induce integrin α L β 2-mediated slow leukocyte rolling. *Blood* 2010;116:485–94. doi:10.1182/blood-2009-12-259556.

49. Hidalgo A, Peired AJ, Wild M, Vestweber D, Frenette PS. Complete identification of E-selectin ligands on neutrophils reveals distinct functions of PSGL-1, ESL-1, and CD44. *Immunity* 2007;26:477–89. doi:[10.1016/j.immuni.2007.03.011](https://doi.org/10.1016/j.immuni.2007.03.011).
50. Panés J, Granger DN. Leukocyte–endothelial cell interactions: molecular mechanisms and implications in gastrointestinal disease. *Gastroenterology* 1998;114:1066–90. doi:[10.1016/s0016-5085\(98\)70328-2](https://doi.org/10.1016/s0016-5085(98)70328-2).
51. Zundler S, Fischer A, Schillinger D, et al. The $\alpha 4\beta 1$ homing pathway is essential for ileal homing of Crohn's disease effector T cells in vivo. *Inflamm Bowel Dis* 2017;23:379–91. doi:[10.1097/MIB.0000000000001029](https://doi.org/10.1097/MIB.0000000000001029).
52. Becker E, Dedden M, Gall C, et al. Residual homing of $\alpha 4\beta 7$ -expressing $\beta 1+\text{PII}6+$ regulatory T cells with potent suppressive activity correlates with exposure-efficacy of vedolizumab. *Gut* 2022;71:1551–66. doi:[10.1136/gutjnl-2021-324868](https://doi.org/10.1136/gutjnl-2021-324868).
53. Schweda A, Becker E, Wiendl M, et al. Etrolizumab-s does not induce residual trafficking of regulatory T cells. *Inflamm Bowel Dis* 2022;28:1746–55. doi:[10.1093/ibd/izac137](https://doi.org/10.1093/ibd/izac137).

Can we simplify the journey in UC?



JYSELECA is a once-daily oral treatment* that provides rapid** and long-term† efficacy up to ~4 years¹⁻³

Helping patients return to their normal lives^{4††}

Discover more

[Full Prescribing information.](#) [Report an adverse event.](#)

* Recommended dose for induction and maintenance is 200 mg once daily.¹ JYSELECA is not recommended in patients aged 75 years and older as there is no data in this population; in patients aged 65 years and over the recommended dose is 200 mg once daily for induction treatment and 100 mg daily for maintenance treatment.¹

** Data from a *post-hoc* analysis of diary data from the double-blind, randomised, placebo-controlled 58-week SELECTION trial. Achievement of stool frequency subscore of ≤ 1 by Day 3 in biologic-naïve patients, and rectal bleeding subscore of 0 by Day 5 in biologic-experienced patients.²

† Interim analysis of SELECTIONLTE assessing the efficacy and safety of open-label JYSELECA 200 mg through LTE Week 144 in completers and LTE Week 192 in non-responders, respectively, representing a total of 3.9 years of treatment each (completers: 58 + 144 weeks; non-responders 10 + 192 weeks).³

†† Determined in a *post-hoc* exploratory analysis of the SELECTION trial assessing HRQoL and the comprehensive disease control multi-component endpoint, which comprises both clinical and QoL outcomes, in individuals receiving JYSELECA (n=786).⁴ Each patient has their own definition of normal life.

▼ This medicine is subject to additional monitoring.

HRQoL, Health-related quality of life; LTE, Long term extension; QoL, Quality of life; UC, Ulcerative colitis.

1. JYSELECA Summary of Product Characteristics, January 2024.
2. Danese S, et al. *Am J Gastroenterol* 2023;118(1):138–147.
3. Feagan BG, et al. *ECCO* 2023; #OP35.
4. Schreiber S, et al. *J Crohns Colitis* 2023;17(6):863–875.